Acute Morphine, Chronic Morphine, and Morphine Withdrawal Differently Affect Pleiotrophin, Midkine, and Receptor Protein Tyrosine Phosphatase β/ζ Regulation in the Ventral Tegmental Area

Daniel García-Pérez[1,2] · M. Luisa Laorden[1,2] · M. Victoria Milanés[1,2]

Abstract Pleiotrophin (PTN) and midkine (MK) are secreted growth factors and cytokines, proposed to be significant neuromodulators with multiple neuronal functions. PTN and MK are generally related with cell proliferation, growth, and differentiation by acting through different receptors. PTN or MK, signaling through receptor protein tyrosine phosphatase β/ζ (RPTPβ/ζ), lead to the activation of extracellular signal-regulated kinases (ERKs) and thymoma viral proto-oncogene (Akt), which induce morphological changes and modulate addictive behaviors. Besides, there is increasing evidence that during the development of drug addiction, astrocytes contribute to the synaptic plasticity by synthesizing and releasing substances such as cytokines. In the present work, we studied the effect of acute morphine, chronic morphine, and morphine withdrawal on PTN, MK, and RPTPβ/ζ expression and on their signaling pathways in the ventral tegmental area (VTA). Present results indicated that PTN, MK, and RPTPβ/ζ levels increased after acute morphine injection, returned to basal levels during chronic opioid treatment, and were upregulated again during morphine withdrawal. We also observed an activation of astrocytes after acute morphine injection and during opiate dependence and withdrawal. In addition, immunofluorescence analysis revealed that PTN, but not MK, was overexpressed in astrocytes and that dopaminergic neurons expressed RPTPβ/ζ. Interestingly, p-ERK 1/2 levels during chronic morphine and morphine withdrawal correlated RPTPβ/ζ expression. All these observations suggest that the neuroprotective and behavioral adaptations that occur during opiate addiction could be, at least partly, mediated by these cytokines.

Keywords Opiate dependence · Reward pathway · Pleiotrophin · Midkine · Glial fibrillary acidic protein

Abbreviations

PTN	Pleiotrophin
MK	Midkine
RPTPβ/ζ	Receptor protein tyrosine phosphatase β/ζ
VTA	Ventral tegmental area
GFAP	Glial fibrillary acidic protein
GFAP-IR	GFAP immunoreactivity
DA	Dopamine

✉ Daniel García-Pérez
daniel.garcia9@um.es

1   Group of Cellular and Molecular Pharmacology, Department of Pharmacology, University of Murcia, Campus de Espinardo, 30100 Murcia, Spain

2   IMIB, Instituto Murciano de Investigación Biosanitaria, Murcia, Spain

Introduction

Astrocytes perform numerous functions: they provide structural support for nerve cells, modulate the environment around neurons, regulate the production of synapses, maintain the blood–brain barrier, and release a range of neuronal growth factors [1, 2]. Since glia play a variety of roles in the central nervous system (CNS), a stimulus that affects their morphology and function has widespread consequences including changes in neurotransmission, metabolism of neurotransmitters, synaptic plasticity, and propagation of action potentials [2]. Morphine administration is established as a stimulus that affects glial activity. For example, morphine administration

induces region-specific upregulation of glial fibrillary acidic protein (GFAP), a protein constituent found specifically in astrocytes, in specific brain areas [3]. Interestingly, evidence has demonstrated that tolerance and dependence are associated with opioid-induced increases in glial cell activity, resulting in neuroadaptations that may directly contribute to the reinforcing effects of these agonists [4].

Activation of astrocytes induces the synthesis and release of substances capable of modulating the surrounding cells (including neurons) like neurotransmitters, neurotrophic factors, cytokines, chemokines, and extracellular matrix factors [5–7]. Morphine not only increases glial activation but also the consequent production of immune factors (chemokines and cytokines) [8]. In addition, some of these molecules exhibit a profile similar to that of neuromodulators or behave like neurotrophic factors [9, 10]. These data raise the possibility that astrocytes contribute to the synaptic plasticity during the development of drug addiction. Moreover, cytokines, in addition to dopamine (DA) and neurotrophins, have been proposed as key mediators of addiction-related neuronal plasticity [11].

Pleiotrophin (PTN) is a secreted cell signaling cytokine that acts as growth factor and as a neuromodulator with multiple neuronal functions [12]. PTN shares high homology with another peptide, denominated Midkine (MK) [13]. PTN and MK have been involved in neurodegenerative disorders and in response to chronic drug consumption. PTN is upregulated in the cortex and caudate putamen after injection of a cannabinol [14], and in NAc after acute administration of amphetamine [15]. Likewise, increased mRNA and protein levels were found in the prefrontal cortex of alcoholics and smokers [16]. In addition, PTN is also highly upregulated in substantia nigra of patients with Parkinson disease [17] and treatment with L-Dopa increases PTN levels in the striatum [18]. Given that these cytokines exert effects that are similar to those of neurotrophins, these findings support the hypothesis that these two cytokines are upregulated in order to induce neurotrophic or neuroprotective effects during drug consumption [19]. Different membrane receptors could function as a multi-molecular complex coordinated to transduce the PTN-MK signal into the cell by different signaling pathways [12]. So, PTN and MK bind common receptors, including receptor protein tyrosine phosphatase β/ζ (RPTPβ/ζ) [20], which is abundantly expressed in the CNS. The interaction of MK or PTN with RPTPβ/ζ establishes a "ligand-dependent inactivation" of RPTPβ/ζ, presumably a consequence of RPTPβ/ζ dimerization [21]. As a consequence, PTN or MK signaling through RPTPβ/ζ leads to activation of ERK and phosphatidylinositol 3-kinase (PI3K)-Akt [22, 23], important axes inducing morphological changes and modulating addictive behaviors.

To date, despite the fact that morphine causes a full addiction syndrome and persistent restructuring in the mesolimbic reward system, the role of PTN and MK in the context of morphine administration has only been assessed in morphine-induced

antinociceptive effects [24, 25]. The action of many addictive substances converges on the mesolimbic dopaminergic reward pathway, inducing increased firing of dopaminergic neurons in the ventral tegmental area (VTA) of the midbrain [26, 27]. Importantly, in preliminary work from our group [28], RT-PCR analysis detected that PTN and MK in the VTA were altered under different paradigms of morphine administration. These preliminary results prompted us to study if these changes were also observed at the protein level. Given the important implications of DA neurotransmission in addiction disorders and the complexity of opiate-induced neuroadaptive responses in the brain reward dopaminergic system, the present study was focused on identifying whether the expression of PTN, MK, RPTPβ/ζ, and their intracellular signaling pathways (Akt and ERK) are altered in association with acute and chronic morphine exposure as well as with morphine withdrawal in the VTA. Then, we assessed the possible activation of astrocytes, which could lead to the release of astrocyte-related soluble factors. Finally, we also aimed to identify those cell subpopulations that produced and secreted PTN and/or MK and those that expressed RPTPβ/ζ in response to morphine administration or morphine withdrawal.

Materials and Methods

Subjects

Male Wistar rats ($n = 65$; Harlan, Barcelona, Spain) initially weighing 220–240 g were housed (2–3/cage) on arrival in a room with controlled temperature (22 ± 2 °C) and humidity (50 ± 10 %), with free access to water and food (Harlan Teklad standard rodent chow; Harlan Interfauna Ibérica, Barcelona, Spain). Animals were adapted to a standard 12 h light–dark cycle (lights on 08:00 h to 20:00 h) for 7 days before the beginning of the experiments. All surgical and experimental procedures were performed in accordance with the European Communities Council Directive of 24 November 1986 (86/609/EEC) and were approved by the local Committees for animal research (REGA ES300305440012).

Drug Treatment and Experimental Procedure

Following habituation, rats were implanted subcutaneously (s.c.) with placebo pellets (lactose) for 6 days. Another set of rats were made dependent on morphine by implantation (s.c.) of two 75 mg morphine pellets under light ether anesthesia. This procedure has been shown to produce consistent plasma morphine concentrations beginning a few hours after the implantation of the pellets and a full withdrawal syndrome after acute injection of opiate antagonists [29]. On day 7, rats were injected intraperitoneally (i.p.) with either morphine HCl (20 mg/kg; in a volume of 1 ml/kg body weight), naloxone (1 mg/kg; 1 ml/kg body weight), or an

equivalent volume of 0.9 % saline and sacrificed 2 h later. There were five experimental groups: chronic placebo + acute saline, chronic placebo + acute morphine, chronic morphine + acute saline, chronic placebo + acute naloxone, and chronic morphine + acute naloxone. The weight gain of the rats was checked during chronic treatment to ensure that the morphine was liberated correctly from the pellets because it is known that chronic morphine treatment induces a decrease in body weight gain due to lower caloric intake [30]. In addition, the animals were observed for opioid withdrawal behaviors for 30 min before and after naloxone injection.

Electrophoresis and Western Blotting

Animals were killed by rapid decapitation. The brains were removed, placed (with its ventral surface facing up) on a plaque over crushed ice, and tissue samples of the VTA were dissected out as described in [31]. Brain regions were placed in individual wells, frozen immediately on dry ice, and stored at −80 °C until assaying. Samples were placed in homogenization buffer, homogenized, and sonicated for 30 s prior to centrifugation at 10,000×g for 10 min at 4 °C. Samples containing equal quantities of total proteins (20–40 mg, depending on the protein of interest) were separated by 6, 10, or 12 % SDS-PAGE (depending on the molecular weight of the protein of interest) and transferred onto PVDF membranes (Millipore, Billerica, MA, USA). Membranes were blocked in TBS containing 0.15 % Tween-20 (TBS-T), 1 % BSA for 90 min at room temperature (RT), and incubated overnight at 4 °C with the primary antibody diluted in 1 % BSA in TBS-T. The following primary antibodies were used: goat polyclonal anti-PTN (1:1000; AF-252-PB, R&D Systems, Minneapolis, MN, USA); rabbit polyclonal anti-MK (1:500; sc-20715, Santa Cruz Biotechnology, Santa Cruz, CA, USA); mouse monoclonal anti-RPTPβ/ζ, (1:750; 610180, BD Transduction Laboratories, Erembodegem, Belgium); mouse monoclonal anti-phospho-ERK 1/2 (p-ERK 1/2; 1:1000; sc-7383; Santa Cruz Biotechnology); mouse monoclonal anti-ERK 1/2 (1:1000; sc-135900; Santa Cruz Biotechnology); rabbit monoclonal anti-phospho-Akt (p-Akt; 1:2000; #4060, Cell Signaling Technology Inc., Danvers, MA, USA); rabbit polyclonal anti-Akt (1:1000; #9272, Cell Signaling Technology Inc.). Blots were washed and incubated for 90 min at RT in TBS-T with 1 % BSA with appropriate horseradish peroxidase (HRP) conjugated secondary antibodies: anti-rabbit (1:5000; sc-2004, Santa Cruz Biotechnology) anti-mouse (1:5000; sc-2005, Santa Cruz Biotechnology), or anti-goat (1:5000; sc-2350, Santa Cruz Biotechnology). After washing, immunoreactivity was detected with an enhanced chemiluminescent/chemifluorescent western blot detection system (ECL Plus; GE Healthcare, UK) and visualized by a Typhoon 9410 variable mode Imager (GE Healthcare). We used GAPDH or α-Tubulin as our loading control. Before reprobing, blots were

stripped by incubation with stripping buffer (glycine 25 mM and SDS 1 %, pH 2) for 1 h at 37 °C. Blots were subsequently reblocked and probed with rabbit polyclonal anti-GAPDH (1:5000; #2118, Cell Signaling Technology Inc.) or rabbit polyclonal anti-α-Tubulin (1:2500; #2144, Cell Signaling Technology Inc.). For Akt or ERK experiments, the same membrane was processed in the following order: incubation with anti-p-Akt or anti-p-ERK 1/2 antibody, stripping, incubation with anti-Akt or anti-ERK antibody, and stripping and incubation with anti-GAPDH antibody. The ratios of PTN/GAPDH, MK/GAPDH, RPTPβ/ζ/α-Tubulin, p-Akt/t-Akt, t-Akt/GAPDH, p-ERK 1/t-ERK 1, t-ERK 1/GAPDH, p-ERK 1/GAPDH, p-ERK 2/t-ERK 2, t-ERK 2/GAPDH, and p-ERK 2/GAPDH were plotted and analyzed. Protein levels were corrected for individual levels.

Brain Perfusion and Sectioning

Another set of rats were deeply anesthetized with an overdose of pentobarbital (100 mg/kg i.p.) and perfused transcardially with saline followed by fixative containing paraformaldehyde (4 % paraformaldehyde in 0.1 M borate buffer, pH 9.5). After removal of the perfused brains, they were post-fixed in the same fixative for 3 h and stored at 4 °C in PBS containing 30 % sucrose until coronal sections (30 μm thickness) were cut rostrocaudally on a freezing microtome (Leica, Nussloch, Germany). The atlas of Paxinos and Watson (2007) [32] was used to identify the VTA. The sections were cryoprotected and stored at −20 °C until use.

GFAP Immunohistochemistry

Sections of the VTA were used for immunohistochemistry to detect astrocytes. Brain sections were rinsed in PBS and an antigen retrieval procedure was applied by treating sections with citrate buffer (10 mM citric acid in 0.05 % Tween 20, pH 6.0) at 60 °C for 20 min. Endogenous peroxidase activity was inhibited with 0.3 % H_2O_2 and non-specific binding sites were blocked in 3 % normal goat serum (Sigma, USA)/0.3 % Triton X-100 in PBS for 1 h at RT. The sections were incubated for 72 h (4 °C, constant shaking) with primary antibody/mouse monoclonal anti-GFAP (1:400; sc-33673, Santa Cruz Biotechnology). The sections were then incubated for 2 h at RT in biotinylated secondary antibody/anti-mouse (1:500; BA-2000, Vector Laboratories, Burlingame, CA, USA). Tissue was processed by the avidin-biotin immunoperoxidase method (1:250; Vectastain ABC Elite Kit, Vector Laboratories) and immunopositive cells were visualized by addition of the chromogen 3,3′-diaminobenzidine tetrahydrochloride (DAB; Sigma, USA) and 0.005 % H_2O_2. Sections were mounted on chrome-alum gelatin-coated slides and dehydrated in graded ethanol series and xylene before being coverslipped.

Quantification GFAP-Positive Cells

Neuroanatomical sites were identified using the Paxinos and Watson (1997) atlas. Photomicrographs were captured by means of Leica microscope (DM 4000B; Leica) connected to a video camera (DFC290; Leica). GFAP-positive cell nuclei were counted using a computer-assisted image analysis system (QWIN; Leica). Positive cells were counted at ×20 magnification. A square field (325 μm) was superimposed upon captured image to use as reference area. The number of astrocytes was counted bilaterally in four to five sections from each animal, and averaged to obtain a single value for each rat. The whole histological quantification was performed blindly. Total counts for different brain regions are expressed as mean ± SEM.

GFAP Densitometric Analysis

The same conventional light microscopy described above was used for optical density (OD) study of the nuclei and processes. Photomicrographs were captured at ×10 magnification (image size, 936 × 702 μm). To avoid observer bias, all sections were quantified by a blinded investigator. The intensity of the different brain areas was evaluated through densitometric analysis using ImageJ 1.43 software (NIH ImageJ, Bethesda, MD, USA). The region of interest was outlined in each image, and a mean optical density value was obtained. Background was determined from unstained areas in the tissue section. The corrected densitometric signal was calculated by subtracting the background from each densitometric determination. Four to five sections from each animal were evaluated. A mean value for different regions of each animal was then obtained. The area outlined in each image was also calculated to assure that there were no differences between the regions of interest analyzed in different groups.

Immunofluorescence

Triple immunofluorescence study was carried out to detect GFAP, PTN, and MK. Sections were treated with citrate buffer (60 °C for 20 min). Non-specific Fc binding sites were blocked with 2 % normal horse serum/0.3 % Triton X-100 in PBS for 1 h at RT, and the sections were incubated for 72 h (4 °C, constant shaking) with primary antibodies/mouse monoclonal anti-GFAP (1:400; sc-33673, Santa Cruz Biotechnology), goat polyclonal anti-PTN (1:400; AF-252-PB, R&D Systems), and rabbit polyclonal anti-MK (1:250; sc-20715, Santa Cruz Biotechnology). Secondary antibodies were applied sequentially for 4 h: Alexa Fluor 488 anti-rabbit IgG (1:1000; A-21206, Invitrogen, Eugene, OR, USA), Alexa Fluor 594 anti-goat IgG (1:1000; A-11058, Invitrogen), and Alexa Fluor 405 anti-mouse IgG (1:1000; A-31553, Invitrogen). After washing, the sections were mounted in ProLong® Gold antifade reagent (Invitrogen).

Double-fluorescent labeling was processed as previously explained. Mesencephalic sections were incubated (72 h, 4 °C) with mouse monoclonal anti-RPTPβ/ζ (1:50; 610180, BD Transduction Laboratories) and goat polyclonal anti-tyrosine hydroxylase (TH; 1:4000; ab101853, Abcam, Cambridge, UK) to identify midbrain dopaminergic neurons. Appropriate secondary antibodies were used: Alexa Fluor 488 anti-goat IgG (1:1000; A-11055, Invitrogen) and Alexa Fluor 594 anti-mouse IgG (1:1000; A-21203, Invitrogen). Sections were incubated in DAPI (1:100,000) for 1 min, and mounted in ProLong® Gold antifade reagent (Invitrogen).

Confocal Analysis

The brain sections were examined using a Leica DMIRE2 confocal microscope and Leica Confocal Software (Leica Microsystems). Images were captured from low magnification to high magnification (×20 to ×63 oil objective). Confocal images were obtained using 405-nm excitation for Alexa Fluor 405 or DAPI, 488-nm excitation for Alexa Fluor 488, and 543-nm excitation for Alexa Fluor 594. Emitted light was detected in the range of 450 nm for DAPI, 515–530 nm for Alexa Fluor 488, and 605 nm for Alexa Fluor 594. Every channel was captured separately to avoid spectral crosstalking. A series of optical sections were performed determining an upper and lower threshold using the Z/Y position for Spatial Image Series setting. The optical series covered 20 μm of thickness through the tissue. Images were deconvolved using Huygens Essential 3.6 by Scientifica Volume Imaging (SVI, Hilversum, The Netherlands).

Materials

Morphine HCl and morphine base were supplied from Alcaliber Laboratories (Madrid, Spain) in cooperation with the Área de Estupefacientes y Psicotropos, Agencia Española del Medicamento y de Productos Sanitarios (Madrid, Spain). Naloxone HCl was purchased from Sigma-Aldrich (Sigma Chemical Co, St Louis, MO, USA). Morphine HCl and naloxone HCl doses are expressed as the weight of the salt. Protease inhibitors were purchased from Boehringer Mannheim (Mannheim, Germany); phosphatase inhibitor Cocktail Set was purchased from Calbiochem (Darmstadt, Germany). Morphine HCl and naloxone were prepared fresh each day by reconstitution in sterile saline (0.9 % NaCl; ERN Laboratories, Barcelona, Spain).

Statistical Analysis

Data are presented as mean ± standard error of the mean (SEM). Data were analyzed using one-way or two-way analysis of variance (ANOVA) followed by a post hoc Newman–Keuls test. Correlations between changes in protein expression were assessed using Pearson correlation. Differences

with a $p < 0.05$ were considered significant. Statistical analyses were performed with GraphPad Prism 5 (GraphPad Software Inc., San Diego, CA, USA).

Results

PTN and MK Were Upregulated in the VTA After Morphine Administration and During Precipitated Morphine Withdrawal

PTN and MK have been found to be upregulated in different brain areas after amphetamine, alcohol, or delta-9-tetrahydrocannabinol administration (see "Introduction" section); however, their possible alteration after morphine administration or during morphine withdrawal in the mesolimbic pathway has not been determined. This experiment addressed two questions regarding PTN and MK expression. The first was whether acute or chronic morphine treatment was associated with changes in PTN and/or MK in VTA. ANOVA showed a significant effect after acute morphine for PTN ($F_{(2,20)} = 8.656$; $p = 0.0023$) and MK ($F_{(2,19)} = 6.949$; $p = 0.0062$) in the VTA. As shown in Fig. 1a and c, post hoc comparisons showed that acute morphine administration significantly elevated PTN ($p < 0.01$) and MK ($p < 0.05$) expression in the VTA. This elevation was not seen during chronic morphine administration ($p < 0.01$) compared with acute morphine injection. Two-way ANOVA for PTN expression showed a significant effect of pretreatment ($F_{(1,22)} = 7.23$; $p = 0.0134$). Post hoc test revealed that PTN levels in the VTA were increased after naloxone precipitated morphine withdrawal ($p < 0.05$), as shown in Fig. 1b. Two-way ANOVA for MK showed a significant effect of acute naloxone injection ($F_{(1,23)} = 5.885$; $p = 0.0235$) and an interaction between pretreatment and acute treatment ($F_{(1,23)} = 4.516$; $p = 0.0445$). Post hoc test revealed that MK levels in the VTA were increased after naloxone precipitated morphine withdrawal ($p < 0.05$), as shown in Fig. 1d.

As our first goal was to establish whether acute morphine administration, chronic morphine, or morphine withdrawal affects PTN and/or MK VTN expression, it was important to know if VTA expresses RPTPβ/ζ, one of the main receptors for PTN/MK, as well as whether morphine, morphine dependence, and/or morphine withdrawal alter its expression. So, we next used semi-quantitative Western blot to examine whether morphine and or morphine withdrawal affected RPTPβ/ζ expression protein levels. ANOVA showed a significant effect after acute morphine ($F_{(2,17)} = 17.21$; $p < 0.0001$). As shown in Fig. 1e, post hoc comparisons showed that acute morphine administration significantly elevated RPTPβ/ζ ($p < 0.01$) expression. However, there was a decrease in its expression during morphine dependence compared with the control group receiving placebo plus saline ($p < 0.05$) and with acute morphine-treated rats ($p < 0.001$). Two-way ANOVA for RPTPβ/ζ expression showed a significant

effect of chronic pretreatment ($F_{(24)} = 4.29$; $p = 0.0492$) and an interaction between pretreatment and acute treatment ($F_{(1, 24)} = 5.498$; $p = 0.0276$). Post hoc test revealed that RPTPβ/ζ levels in the VTA were decreased in morphine-dependent rats ($p < 0.05$), as compared with the control group (Fig. 1f). No changes were observed in morphine-withdrawn rats.

The body weight loss after saline or naloxone injection to placebo-pelleted and morphine-dependent rats was also recorded as a sign of opiate withdrawal (Fig. 2a). In agreement with our previous results [31], two-way ANOVA revealed that morphine pretreatment ($F_{(1,46)} = 157.4$, $p < 0.0001$), naloxone injection ($F_{(1,46)} = 167.5$, $p < 0.0001$), and the interaction between pretreatment and acute treatment ($F_{(1,46)} = 103.1$, $p < 0.0001$) had a significant effect on body weight loss. Post hoc analysis showed that naloxone injection to morphine-dependent animals significantly increased ($p < 0.001$) body weight loss when compared with the placebo-pelleted group also receiving naloxone and with morphine-treated rats given saline. We next compared the expression of cytokine levels with the severity of the withdrawal syndrome (measured as body weight loss). We did not detect any correlation between MK expression and the withdrawal index (Fig. 2c). In contrast, we observed that PTN expression was significantly correlated with body weight loss after naloxone injection to morphine-dependent rats (Fig. 2b). The data presented here might suggest that PTN is a genetic factor that plays a role in somatic morphine-withdrawal syndrome.

Astrocytes Were Activated by Morphine and Morphine Withdrawal in the VTA

Astrocytes undergo a process of proliferation, morphological changes, and enhancement of GFAP expression, termed the activation of astrocytes or astrogliosis [33]. In this work, we assessed the activation of astrocytes in the VTA by both measuring the number of astrocytes (as the number of GFAP-positive cells) in the different groups and studying the levels of GFAP immunoreactivity (GFAP-IR) by densitometric analysis. ANOVA showed a significant effect of morphine administration for GFAP-positive cells ($F_{(2,12)} = 5.909$; $p = 0.0202$) and GFAP-IR ($F_{(2,14)} = 8.632$; $p = 0.0048$) in the VTA. Post hoc test revealed that acute morphine elevated the number of GFAP-positive cells and GFAP-IR ($p < 0.05$ and $p < 0.01$, respectively) (Fig. 3g, i). In addition, chronic morphine administration also increased GFAP-IR ($p < 0.05$). Two-way ANOVA for GFAP revealed the main effects for chronic pretreatment ($F_{(1, 14)} = 22.16$; $p = 0.0003$), and significant interaction between acute and chronic treatment ($F_{(1,14)} = 10.530$; $p = 0.0059$). We found that precipitated morphine withdrawal significantly increased the number of GFAP-positive cells in the VTA compared with its control group ($p < 0.001$) and with chronic morphine-treated rats receiving saline ($p < 0.01$; Fig. 3h). Two-way ANOVA for GFAP-IR in the VTA revealed the main effect for chronic pretreatment ($F_{(1,16)} = 17.08$; $p = 0.0008$). Post hoc

Fig. 1 PTN, MK, and RPTPβ/ζ protein expression are altered by acute and chronic morphine administration and during morphine withdrawal in the VTA. Over a 7-day period, control (*pla*) and morphine (*mor*)-dependent rats received saline (*sal*), morphine (*mor*; 20 mg/kg i.p.), or naloxone (*nx*; 1 mg/kg s.c.) on day 7 and were sacrificed 2 h later. Semi-quantitative analysis and representative immunoblots of PTN (**a**, **b**), MK (**c**, **d**), and RPTPβ/ζ (**e**, **f**) protein in VTA isolated from rats receiving the above treatments. Each *bar* corresponds to mean ± SEM. Values are expressed as percentage of controls. $^*p < 0.05$, $^{**}p < 0.01$ vs. pla + sal; $^{++}p < 0.01$, $^{+++}p < 0.001$ vs. pla + mor; $^{#}p < 0.05$ vs. pla + nx; $^{&}p < 0.05$ vs. mor + sal
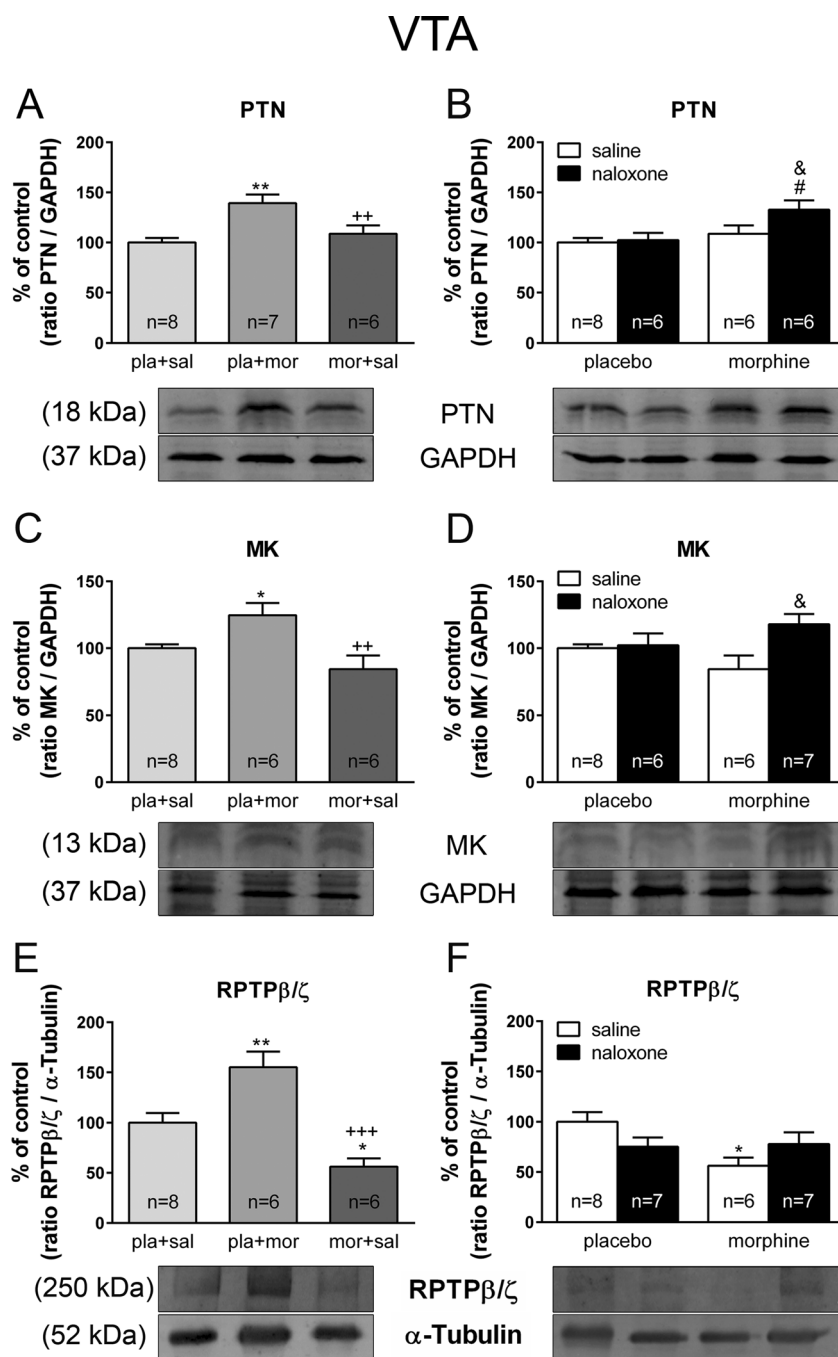
test showed that both chronic morphine and morphine withdrawal elevated ($p < 0.05$) GFAP-IR (Fig. 3j).

PTN but not MK was Overexpressed in Astrocytes During Acute Morphine Administration and Morphine Withdrawal in the VTA

Activation of astrocytes produces the accumulation of intermediate-filament GFAP; consequently, they can be recognized by their stellate morphology. Triple immunofluorescence study revealed that acute morphine (Fig. 4b–b⁗) or morphine

withdrawal (Fig. 4c–c⁗) mediated the activation of astrocytes that expressed high levels of PTN protein, but not MK protein in the VTA. Cells that produced MK are supposed to be neurons due to their size and morphology and the fact that MK and RPTPβ/ζ colocalized (data not shown).

RPTPβ/ζ was Expressed in Midbrain Dopaminergic Neurons

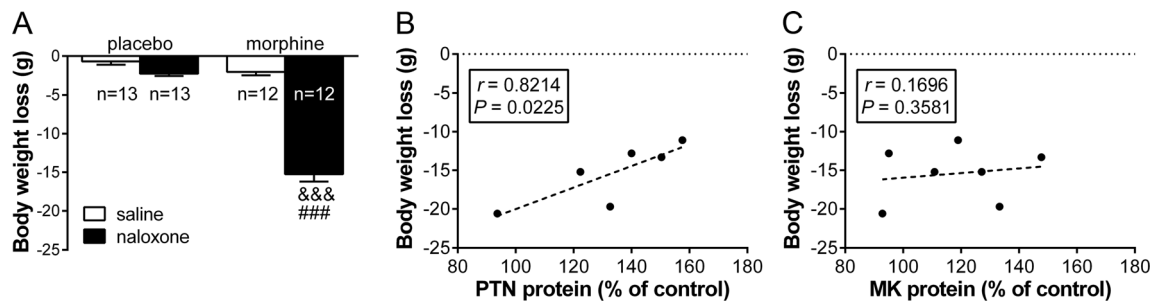RPTPβ/ζ is a transmembrane tyrosine phosphatase, the extracellular domain of which carries chondroitin sulfate chains.

Fig. 2 **a** Effects of naloxone-induced morphine withdrawal on body weight loss. Rats were implanted with morphine or placebo pellets for 7 days. Weight loss was checked immediately before and 2 h after naloxone injection. Data shown are means ± SEM. Post hoc test revealed that there was an increase in body weight loss during morphine withdrawal. $^{###}p < 0.001$ vs. pla + nx; $\&\&\& \ p < 0.001$ vs. mor + sal. **b**, **c** Correlation analysis between PTN or MK and body weight loss. The percent increase in PTN levels was positively correlated with the severity of the withdrawal syndrome

The anti-RPTPβ/ζ antibody used recognizes only the intracellular portion of the RPTPβ/ζ to avoid non-specific labeling of other proteoglycans and especially of phosphacan, a secreted peptide which has the same molecular structure as the extracellular portion of the RPTPβ/ζ.

In order to determine where this receptor is located, we immunolabeled RPTPβ/ζ in combination with specific cell markers on the mesencephalon of morphine-treated rats. At low magnification, we observed that following morphine injection, there was a region-specific increase of RPTPβ/ζ protein in the VTA, but weak or absent staining was detected in the interpeduncular nucleus (IP) or red nucleus (RN) (Fig. 5a–a‴). At high magnification, RPTPβ/ζ immunoreactivity was widely distributed throughout the VTA, and double-labeling with anti-TH (the rate-limiting enzyme of DA synthesis) showed that RPTPβ/ζ is located on cell bodies and proximal processes of almost all dopaminergic neurons in the VTA (Fig. 5c–c‴). There were some RPTPβ/ζ^{+}/TH^{-} cells that might represent GABAergic interneurons in the VTA.

ERK Pathway but not Akt was Activated by Morphine and by Precipitated Morphine Withdrawal in the VTA

In each experiment, the specific signal of p-Akt or p-ERK proteins was normalized to the corresponding Akt or ERK signals, respectively, and then to the level of GAPDH measured in the same preparation. Previously, it has been described that PTN or MK signaling through RPTPβ/ζ leads to activation of ERK and Akt pathways [22, 23]. ANOVA for p-Akt showed a significant effect after acute or chronic morphine administration ($F(2,18) = 5.265$; $p = 0.0175$) failed to detect significant changes in t-Akt expression in the VTA ($F(2,18) = 2.845$; $p = $ ns) (Fig. 6a, c). Post hoc test revealed that p-Akt levels in the VTA were decreased in morphine-dependent rats ($p < 0.05$). Two-way ANOVA revealed that morphine withdrawal had a significant effect on p-Akt ($F(1, 21) = 5.190$; $p = 0.0332$). Post hoc test revealed that p-Akt levels in the VTA were significantly ($p < 0.05$) elevated in morphine-withdrawn rats compared with the morphine-

dependent group receiving saline instead naloxone (Fig. 6b). Two-way ANOVA revealed that morphine pretreatment ($F(1, 21) = 1.83$; $p = 0.0539$), acute naloxone injection ($F(1, 21) = 0.04$; $p = 0.8352$), or the interaction between pretreatment and acute treatment ($F(1,21) = 0.13$; $p = 0.7172$) had no significant effects on t-Akt (Fig. 6d).

Because t-ERK showed changes after the different treatments, p-ERKs 1/2 were quantified by Western blot using both t-ERK and GAPDH as loading controls (Fig. 7). ANOVA showed a significant effect after acute or chronic morphine for p-ERK 1/t-ERK 1 ($F(2,19) = 11.65$; $p = 0.0007$) and for p-ERK 2/t-ERK 2 ($F(2,19) = 15.26$; $p = 0.0002$). As shown in Fig. 7a and g, post hoc comparisons showed that both acute and chronic morphine administration significantly elevated p-ERK 1/t-ERK 1 ($p = 0.001$; $p = 0.01$) and p-ERK 2/t-ERK 2 ($p = 0.001$; $p = 0.001$) expression in the VTA. Two-way ANOVA for p-ERK 1/t-ERK 1 and p-ERK 2/t-ERK 2 expression showed a significant effect for morphine pretreatment (p-ERK 1—$F(1,24) = 21.15$, $p = 0.0001$; p-ERK 2—$F(1,24) = 41$, $p < 0.0001$) and acute naloxone injection (p-ERK 1—$F(1,24) = 4.62$, $p = 0.0419$; p-ERK 2—$F(1,24) = 8.85$, $p = 0.0066$). Post hoc comparisons showed that morphine withdrawal significantly ($p < 0.001$) elevated p-ERK 1 and p-ERK 2 levels compared with their respective controls and with morphine-dependent rats ($p < 0.05$) (Fig. 7b, h). In addition, p-ERK 2 levels were also increased ($p < 0.01$) in morphine-dependent rats compared with its control (Fig. 7h). Similar results were seen by using the p-ERK 1/GAPDH and p-ERK 2/GAPDH. Thus, ANOVA showed a significant effect after acute morphine for p-ERK 1/GAPDH ($F(2,19) = 17.87$; $p < 0.0001$) and after acute and chronic morphine for p-ERK 2/GAPDH ($F(2,19) = 14.91$; $p = 0.0002$). As shown in Fig. 7e and k, post hoc comparisons showed that acute morphine administration injection significantly elevated p-ERK 1/GAPDH and p-ERK 2/GAPDH ($p < 0.001$) as well as and p-ERK 2/GAPDH after chronic morphine treatment ($p < 0.01$) expression in the VTA (Fig. 7k). Two-way ANOVA showed a significant effect of chronic pretreatment for p-ERK 1/GAPDH ($F(1,24) = 12.41$; $p = 0.0017$) and p-
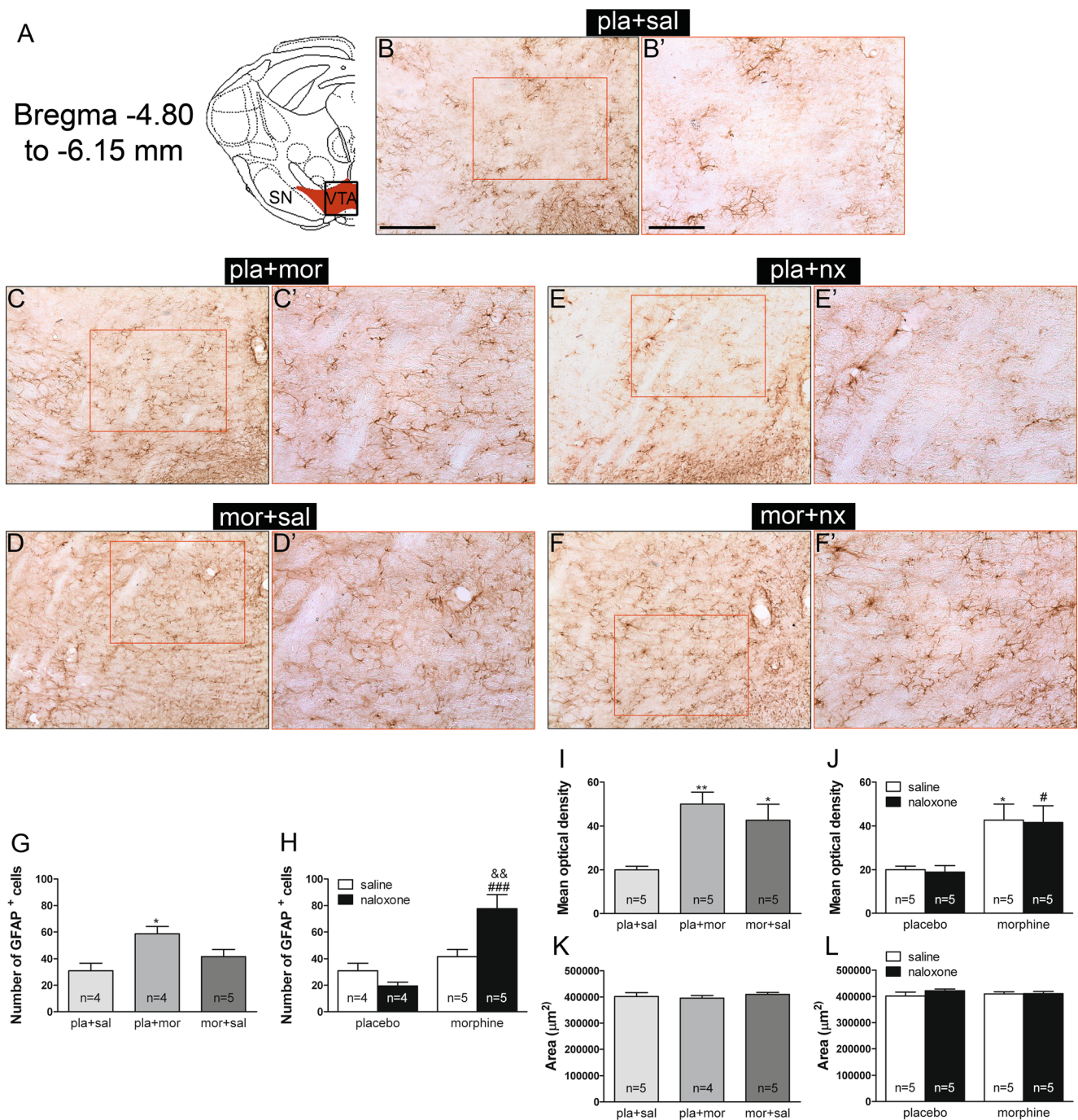
Fig. 3 GFAP expression is enhanced by acute and chronic morphine administration and maintained during morphine withdrawal in the VTA, while astrocyte proliferation only occurs in acute morphine-injected and morphine-withdrawn rats. Over a 7-day period, control (*pla*) and morphine (*mor*)-dependent rats received saline (*sal*), morphine (*mor*; 20 mg/kg i.p.), or naloxone (*nx*; 1 mg/kg s.c.) on day 7 and were sacrificed 2 h later. The analyzed region within the VTA is schematically illustrated in (**a**) (modified from Paxinos and Watson 2007). A *rectangle* indicates the size of the photomicrographs. **b–f** Representative photomicrographs showing immunohistochemical detection of GFAP$^+$ nuclei and fibers in midbrain coronal sections (*scale bar* = 200 μm). **b'–f'** High magnifications from each photomicrograph (*scale bar* = 100 μm). **g, h** Quantitative analysis of astrocytes in the VTA. **i, j** Mean optical density measurement of GFAP immunoreactivity in the VTA from rats receiving the treatments mentioned above. **k, l** Reference area used in the densitometric analysis did not differ between groups. *SN* substantia nigra. Each *bar* corresponds to mean ± SEM. $^*p < 0.05$, $^{**}p < 0.01$ vs. pla + sal; $^#p < 0.05$, $^{###}p < 0.001$ vs. pla + nx; $^{\&\&}p < 0.01$ vs. mor + sal

ERK 2/GAPDH ($F_{(1,24)} = 21.31$; $p = 0.0001$) and acute naloxone injection (p-ERK 1/GAPDH—$F_{(1,24)} = 6.14$, $p = 0.0207$; p-ERK 2/GAPDH—$F_{(1,24)} = 6.81$, $p = 0.0154$). As shown in Fig. 7, there was an increase ($p < 0.01$) of p-
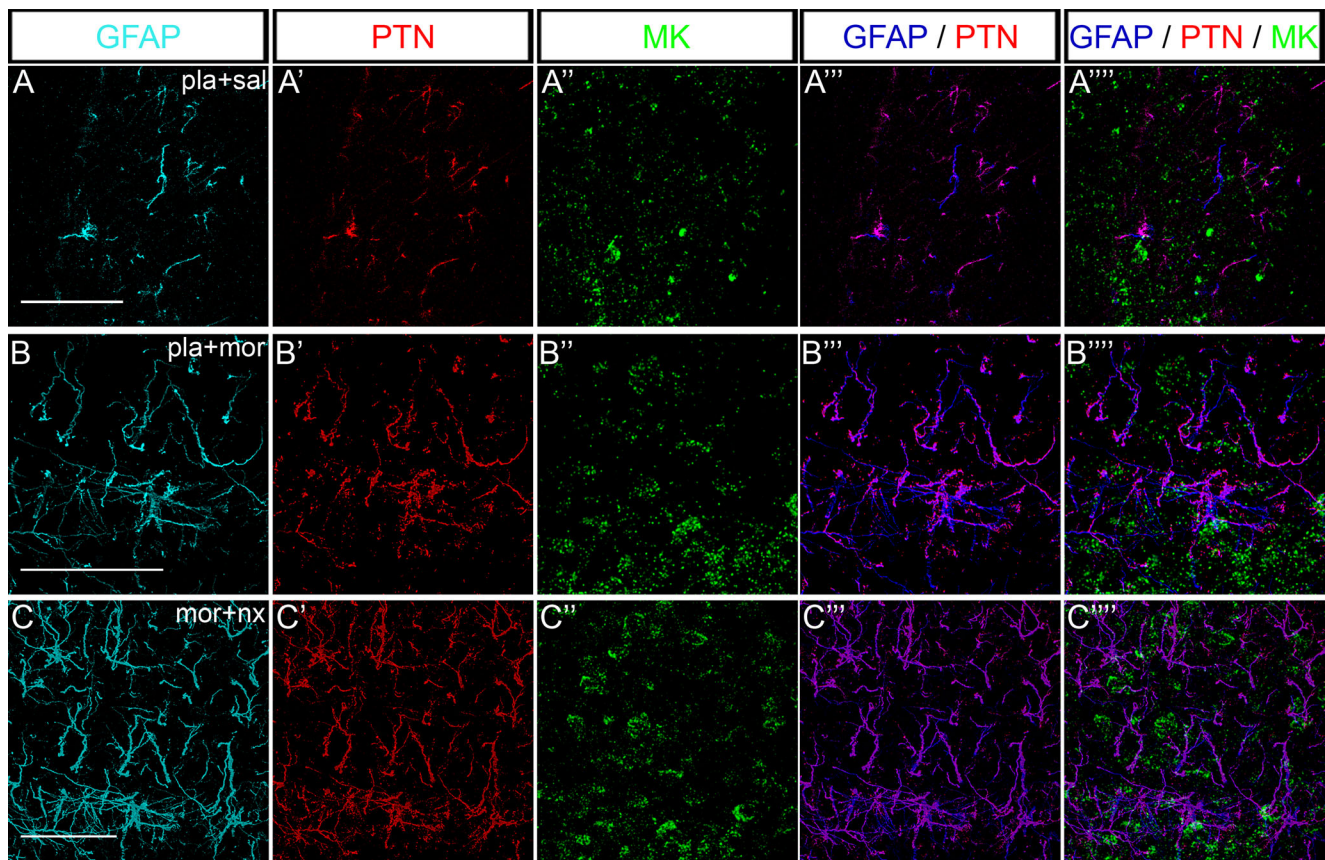
Fig. 4 PTN but not MK is overexpressed in astrocytes during acute morphine administration and morphine withdrawal in the VTA. **a–c** Stack of confocal images from the midbrain areas immunostained for GFAP (*blue*), PTN (*red*), and MK (*green*) in control rats, rats treated with acute morphine, or morphine-dependent animals injected with naloxone. *Scale bar* = **a**–**c**, 50 μm

ERK 1 and p-ERK 2 after naloxone administration to morphine-dependent rats. p-ERK 2 was also elevated during morphine dependence (Fig. 7l).

We next used semi-quantitative Western blot to examine the effect of acute morphine administration, chronic morphine, and morphine withdrawal on t-ERK 1 (ratio t-ERK 1/GAPDH) and t-ERK 2 (ratio t-ERK 2/GAPDH) protein levels (Fig. 7c–j). ANOVA showed significant effects after acute morphine for t-ERK 1 ($F(2,19) = 6.160$; $p = 0.0097$) and for t-ERK 2 ($F(2, 19) = 4.459$; $p = 0.0277$). As shown in Fig. 7c and i, post hoc comparisons showed an increase of t-ERK 1 ($p < 0.01$) and t-ERK 2 ($p < 0.05$) after acute morphine administration. This effect was suppressed in chronic morphine-treated rats. Two-way ANOVA for VTA t-ERK1 and t-ERK2 levels failed to detect any significant effects of chronic morphine pretreatment or morphine withdrawal (Fig. 7d, j).

Relationship Between PTN and RPTPβ/ζ Expression and Between RPTPβ/ζ and ERK Phosphorylated Levels in the Different Experimental Groups

We next compared the expression of PTN and MK with the induction of RPTPβ/ζ protein levels by Pearson correlation. There were no significant correlations in the different experimental groups between MK expression and RPTPβ/ζ protein levels in the VTA (data not shown). In contrast, we observed that during morphine dependence and withdrawal, the expression of PTN was significantly positively correlated with RPTPβ/ζ levels (Fig. 8a–c).

Then we compared the expression of RPTPβ/ζ with the induction of p-ERK protein levels in control rats that were injected an acute dose of morphine. However, RPTPβ/ζ expression in acute morphine-injected rats was not correlated with changes on p-ERK or t-ERK levels. On the other hand, during morphine dependence and withdrawal, expression of RPTPβ/ζ tended to be positively correlated with p-ERK. There was a significant positive correlation between RPTPβ/ζ and both p-ERK 1 and p-ERK 2 protein levels during chronic morphine administration (Fig. 8d, f). As depicted in Fig. 8e and g, a similar trend for positive correlation between RPTPβ/ζ and p-ERK 1/p-ERK 2 was found after naloxone-induced morphine withdrawal.

Discussion

The data presented in this study show that different paradigms of morphine treatment promote a diverse profile of activation of cytokines in the brain. While we observed that a single dose
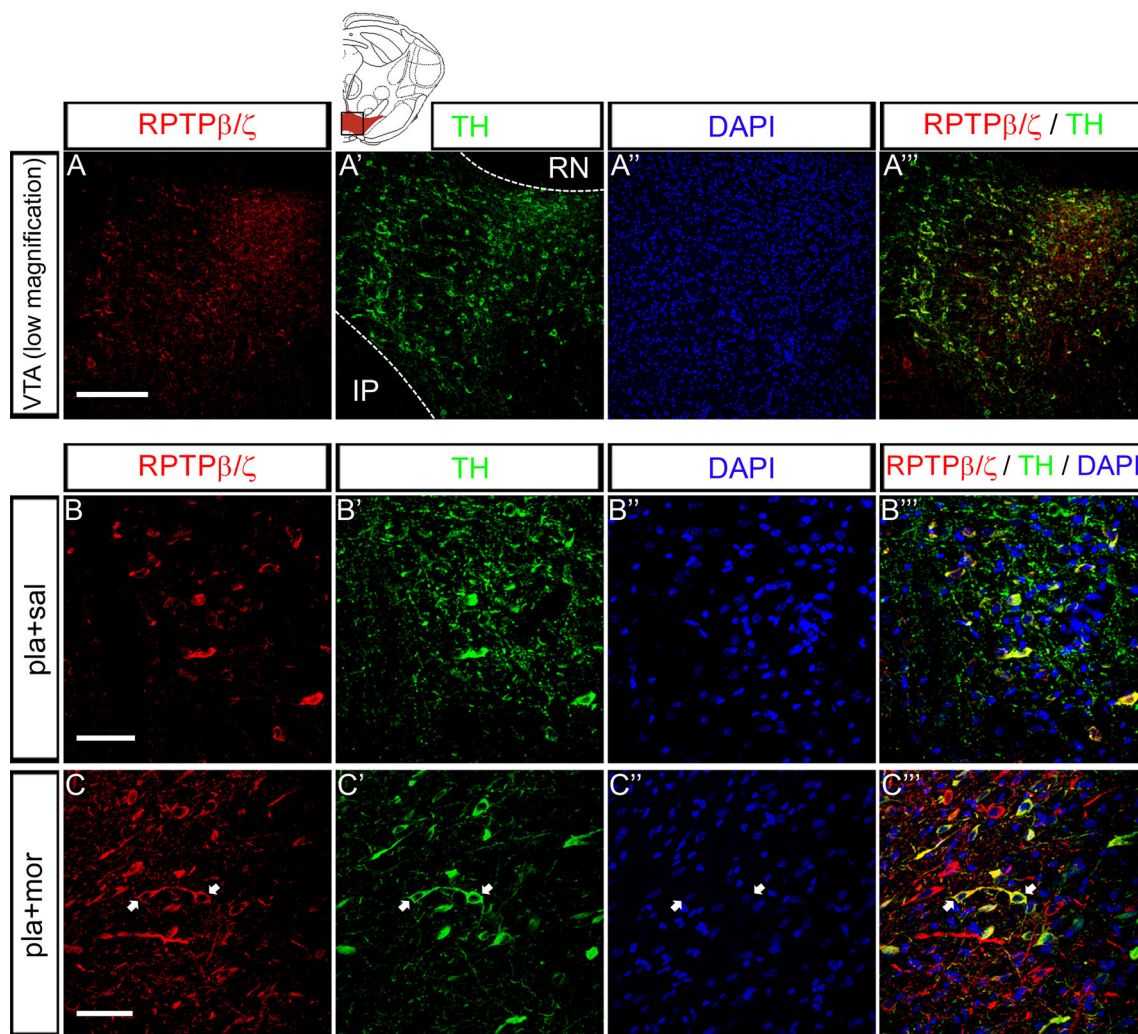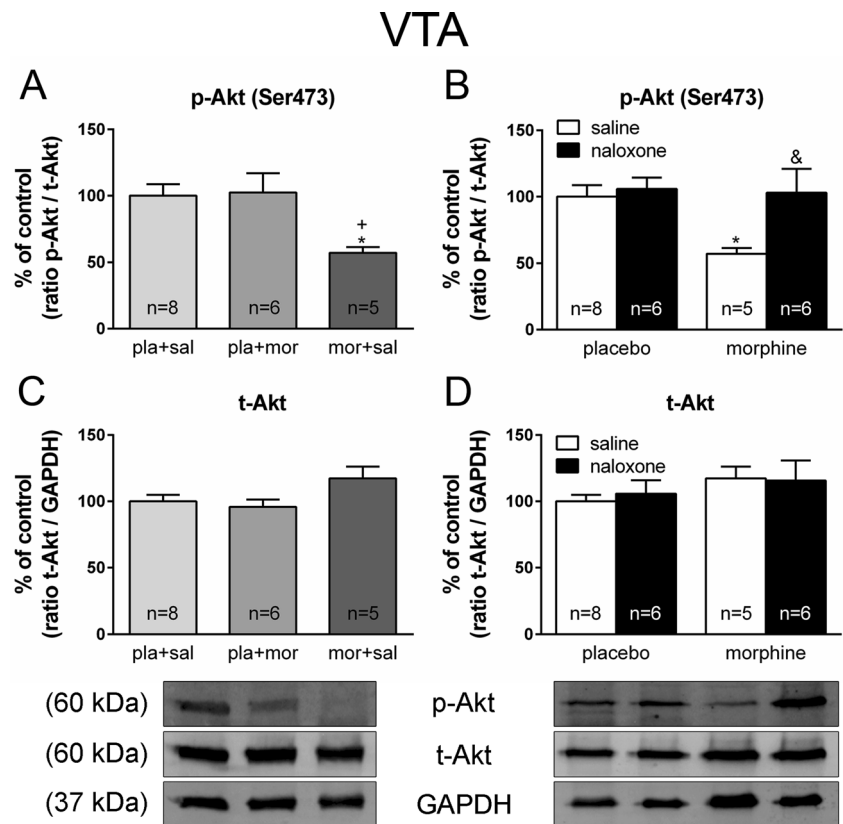
Fig. 5 RPTPβ/ζ is expressed in midbrain dopaminergic neurons. **a** RPTPβ/ζ (*red*) protein in the VTA is region-specific since strong staining in the VTA contrasts with weak or absent staining in the interpeduncular nucleus (IP) or red nucleus (RN). **b**, **c** Stack of confocal images from the midbrain areas in control rats and animals treated with acute morphine. Double-labeling with anti-TH (*green*) showed that, after a morphine challenge, RPTPβ/ζ is located on cell bodies and proximal processes of almost all dopaminergic neurons in the VTA and some non-dopaminergic cells. DAPI (*blue*) was used as a counterstaining in both nuclei. *Scale bar* = **a**, 200 μm; **b**–**c**, 50 μm

of morphine and morphine withdrawal increased the protein levels of PTN and MK in the VTA, chronic morphine administration had the opposite effect since protein levels returned to basal levels or even decreased. Our results are supported by previous findings showing that acute morphine or withdrawal but not chronic morphine promotes the expression of pro-inflammatory cytokines [34]. The present study also showed that PTN up-regulation following morphine administration or during morphine withdrawal is restricted to astrocytes. In agreement with this data, PTN mRNA levels were up-regulated in reactive astrocytes in a model of cryo-injured mouse brain [35]. Besides, in primary cultures of mesencephalon, GFAP-positive astrocytes express PTN mRNA and protein [36], and recently, it has been described that PTN is overexpressed only in astrocytes following an adenoviral vector injection [37]. In contrast, we observed that MK is produced and secreted by non-astrocytic cells following a morphine challenge. Hippocampal pyramidal neurons in adult mouse brain expressed MK, but kainic acid injection induced cell death of pyramidal neurons and enhanced expression of MK by astrocytes [38]. A possible explanation is that, depending on the nature of the insult or the damage/cell death it may produce, MK can be overexpressed by neurons or astrocytes. Moreover, there is evidence that nearly every cell of the CNS, including neurons, is capable of contributing and modifying the central immune signaling [39], for example, by secreting cytokines. For instance, morphine stimulates chemokine CCL2 production by neurons [40]. Cytokines have also been implicated in withdrawal-related behavior. For example, it was showed that corticotrophin releasing factor (CRF) and cytokines work together to worsen ethanol withdrawal phenotypes [41]. Our results indicate that the increase in PTN

expression is related with a less severe withdrawal syndrome, characterized by reduced body weight loss during morphine withdrawal, suggesting that the modulation of PTN signaling pathway might counterbalance the somatic signs of withdrawal. In concordance, it has been described that an augmented withdrawal syndrome score in PTN−/− mice, demonstrating that the lack of endogenous PTN enhances the severity of the physical opiate withdrawal [42]. Although the role of PTN and MK in conditioned place aversion (CPA) remains uncharacterized, future studies should address this issue.

We also found that the expression of PTN− and MK− target receptor (RPTPβ/ζ) was regulated in the same way that these cytokines were regulated by morphine administration. Although the role and the functions of RPTPs are barely characterized, it has been suggested that each of these enzymes has different and specific functions in neurons [43]. Regarding the RPTPβ/ζ signal, we found a staining pattern in neurons. Our results are in line with previous studies where this protein was found to be located in neurons but not in astrocytes [43, 44]. Moreover, TH-positive neurons in primary cultures of mesencephalon have been described to express RPTPβ/ζ [36]. Although it has been reported that adult control rats do not express RPTPβ/ζ in the VTA [45], we detected (by WB and IF) that systemic morphine injection induced RPTPβ/ζ in VTA-dopaminergic neurons in a region-specific manner. Thus, it suggests that RPTPβ/ζ is tightly up-regulated in the VTA after determinate challenges. This expression pattern

supports our hypothesis of an interaction between glial and neuronal function during morphine administration and withdrawal.

Astrocytes can display both hypertrophy and proliferation upon treatment with drugs of abuse. Chronic morphine exposure, achieved by surgically implanted morphine pellets and previously verified to produce opioid tolerance and dependence [46], increased GFAP immunoreactivity in the VTA [3]. This effect was not observed when morphine tolerance and dependence was blocked by concomitant administration of the mu-opioid antagonist, naltrexone [3]. Accordingly, in the present study, acute and chronic morphine caused a robust activation of astrocytes, as evidenced by an increase in the level of GFAP-IR in the VTA, while morphine withdrawal maintained the increase in GFAP-IR levels. Regarding proliferation, repeated methamphetamine administration induces proliferation of astrocytes in rodent striatum and SN [47, 48]. Moreover, morphine and opioid signaling have been shown to promote proliferation of astroglia in the postnatal brain [49]. We observed a rapid astrocyte proliferation in the VTA, the brain area where the rewarding properties of morphine are believed to be firstly mediated (via binding to mu-opioid receptors located on inhibitory neurons) [50]. A question that arises is whether glial activation (measured as GFAP-IR) observed during chronic morphine is maintained throughout a longer time or, on the contrary, it slowly decreases. Data supporting this
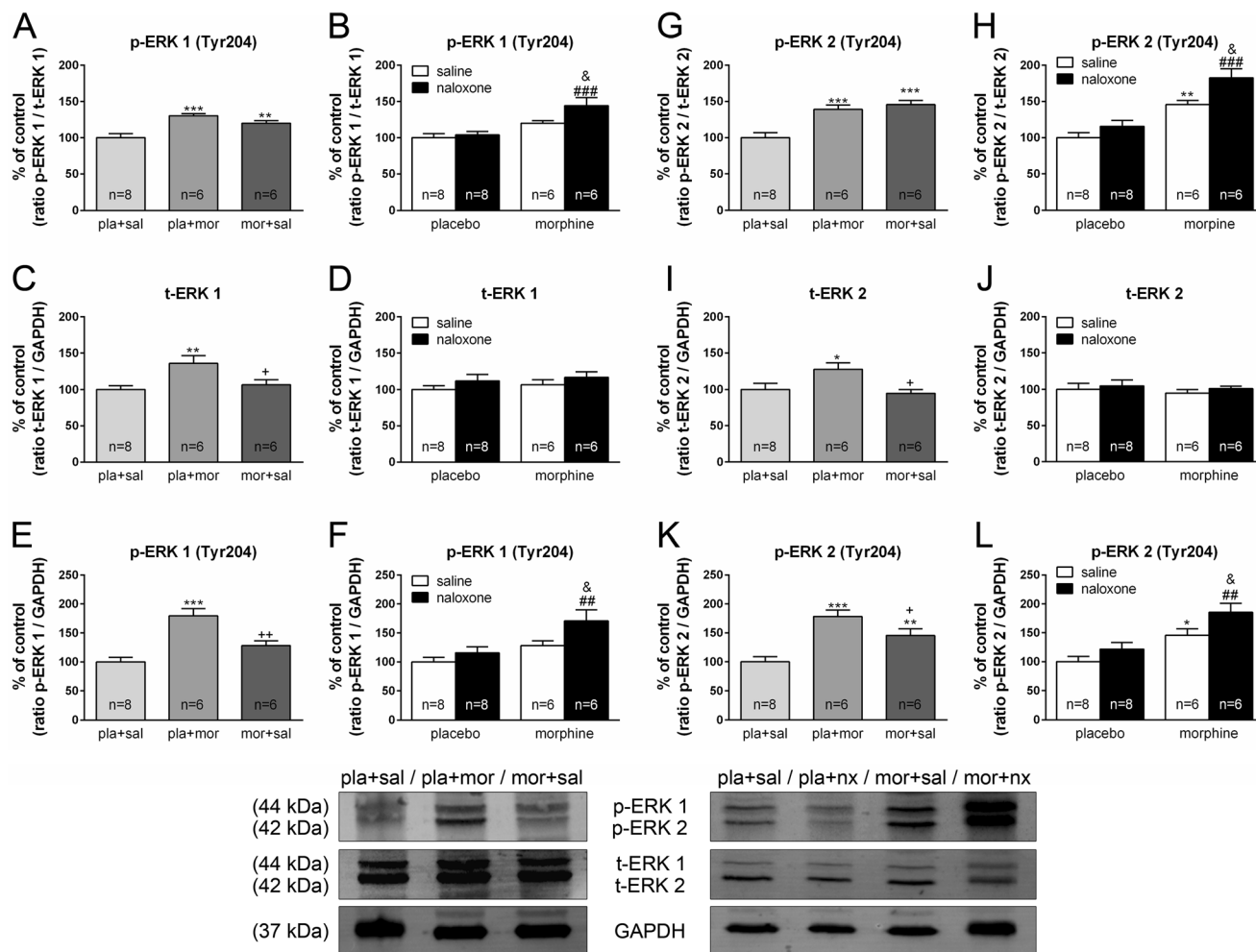
VTA

Fig. 7 p-ERK/t-ERK ratio, t-ERK levels, and p-ERK absolute levels are altered by acute and chronic morphine administration and during morphine withdrawal in the VTA. Over a 7-day period, control (*pla*) and morphine (*mor*)-dependent rats received saline (*sal*), morphine (*mor*; 20 mg/kg i.p.), or naloxone (*nx*; 1 mg/kg s.c.) on day 7 and were sacrificed 2 h later. Semi-quantitative analysis and representative immunoblots of p-ERK 1/t-ERK 1 ratio (**a**, **b**), t-ERK 1 levels (**c**, **d**), p-

ERK 1 absolute levels (**e**, **f**), p-ERK 2/t-ERK 2 ratio (**g**, **h**), t-ERK 2 levels (**i**, **j**), and p-ERK 2 absolute levels (**k**, **l**) in VTA isolated from rats receiving the above treatments. Each *bar* corresponds to mean ± SEM. Values are expressed as percentage of controls. $^*p < 0.05$, $^{**}p < 0.01$, $^{***}p < 0.001$ vs. pla + sal; $^+p < 0.05$, $^{++}p < 0.01$ vs. pla + mor; $^{\#\#}p < 0.01$, $^{\#\#\#}p < 0.001$ vs. pla + nx; $^\&p < 0.05$ vs. mor + sal

second hypothesis is the evidence that, after 2 months, meth-amphetamine induced a long-lasting astrocytic activation and behavioral sensitization, while morphine produced a reversible activation of astrocytes and a reversibility of behavioral sensitization [51].

PTN and MK have been involved in the regulation of the survival and function of dopaminergic neurons [52, 53]. In addition, many reports attribute neuroprotective roles against drug-induced neurotoxicity to these two cytokines. For instance, amphetamine-induced loss of dopaminergic fibers in the striatum was enhanced in PTN knockout (PTN−/−) mice and even caused dopaminergic cell loss in the substantia nigra (SN) of PTN−/− mice [47]. It is important to note that moderate glial activation is thought to be neuroprotective, while

exacerbated activation can be deleterious for the brain [54–56]. Accordingly, amphetamine-induced astrocytosis in the nigrostriatal pathway was increased in PTN−/− mice and in MK−/− mice compared to wild-type mice [47, 48, 57]. As exposed above, morphine withdrawal may promote cytokines and other inflammatory responses that have the potential of exacerbating neuronal damage [34]. The increase in pro-inflammatory cytokines may explain why withdrawal causes caspase-3-dependent apoptosis [58]. So, the enhanced expression of PTN and MK that we observed during acute morphine injection and morphine withdrawal can be regarded as a physiological response to prevent the possible neurotoxic effects of morphine, an excessive astrogliosis or pro-inflammatory cytokine release. Moreover, it has been demonstrated that PTN
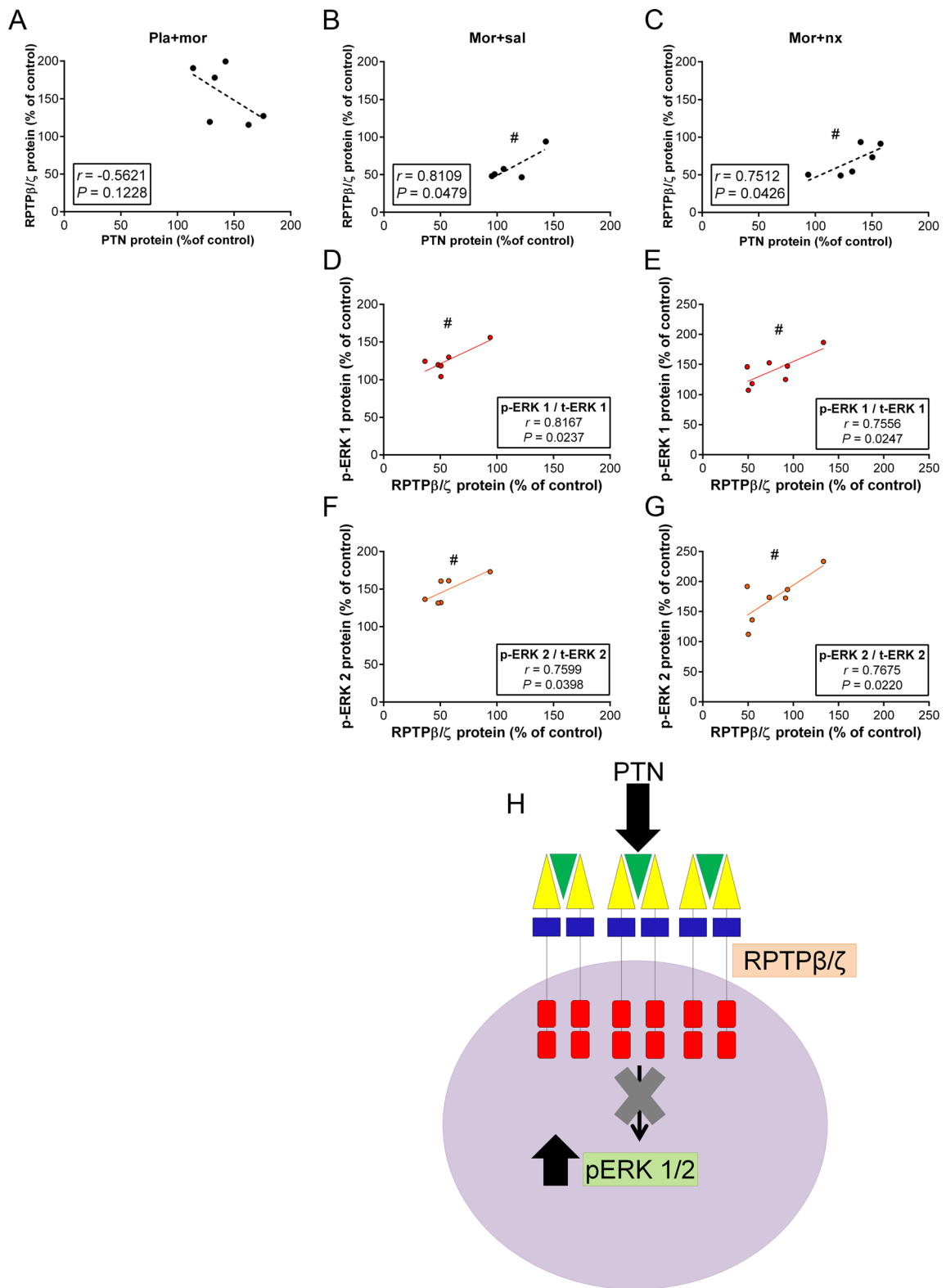
Fig. 8 Correlation analysis between PTN and RPTPβ/ζ expression and between RPTPβ/ζ and ERK phosphorylated levels in the different experimental groups. **a**–**c** The percent increase in PTN levels was positively correlated with RPTPβ/ζ protein during morphine dependence and morphine withdrawal. **d**–**g** During morphine dependence and withdrawal, RPTPβ/ζ expression tended to be positively correlated with p-ERK 1/2 levels. **h** Schematic illustration showing the possible mechanism through which PTN/RPTPβ/ζ signaling may influence ERK phosphorylation during morphine dependence and morphine withdrawal. [#]$p < 0.05$

increases the expression of nuclear receptor related-1 (Nurr1, a transcription factor which is critical for the generation, survival, and maintenance of DA neurons) in neural stem cells to promote production of dopaminergic neurons [52]. Previously, we have observed an increase of Nurr1 after acute morphine administration and withdrawal [31], which parallels that of PTN. So, given the present results, it is tempting to speculate that neuroprotective effects of PTN during acute morphine injection and morphine withdrawal may be, in part, mediated through the induction of Nurr1.

PTN/MK signaling may function through a multi-receptor complex, combining different receptors and most probably other adaptor proteins; then, PTN/MK action over previously mentioned receptors could in turn signal through different signal pathways [12]. It has been documented that the interaction of RPTPβ/ζ with PTN blocks the intrinsic tyrosine phosphatase activity of RPTPβ/ζ [19], leading to an increase in the phosphorylation levels in RPTPβ/ζ target proteins. Interestingly, these target proteins include the PI3K-Akt and Ras-ERK signaling, which have been demonstrated to play a crucial role in opiate addiction (for review see [59]). We detected a direct relationship between PTN and RPTPβ/ζ in morphine-dependent and morphine-withdrawn animals. We propose that PTN expression after chronic morphine and morphine withdrawal would lead to adaptative responses, such as the increase in RPTPβ/ζ levels, which might try to compensate the ligand-dependent inactivation. As exposed above, PTN neuroprotective effects constitute a relevant role, suggesting that PTN signaling pathways are involved in neurodegenerative disorders as well as in response to injuries and chronic drug consumption [12]. On the other hand, several studies have implicated the activation of ERK pathway in drug dependence and naloxone-precipitated withdrawal in different brain areas [60, 61], including the VTA [62, 63]. Interestingly, PTN protective effects against amphetamine-induced toxicity in PC12 cells (which express RPTPβ/ζ and synthesize and release DA) were mediated by the ERK 1/2 signaling pathway [48]. Thus, given the notion that the protection against amphetamine-induced toxicity in vivo and in vitro is mediated by the increased phosphorylation of ERK [47, 48], and our observation of a positive correlation between PTN/RPTPβ/ζ and p-ERK 1/2, we propose that this signaling pathway may be also mediating neuroprotective effects during morphine chronic administration and withdrawal.

On the other hand, a decrease of Akt signaling was detected in the VTA during chronic morphine. This down-regulation is considered critical to mediate the effects of chronic morphine on soma size and electrical excitability [64, 65]. PTN and MK are also known to be neurotrophic factors for DA neurons [36]. Initial up-regulation of PTN promoted regeneration of axons, but subsequent decline in the expression of PTN has been proposed to be responsible for failure to regenerate denervated nerves [66], highlighting the importance of sustained levels of these growth factors to accomplish their trophic function. Nevertheless, we did not find any correlation between PTN, MK, or RPTPβ/ζ and p-Akt levels, so it is reasonable to think that these cytokines do not participate in the decreased dendrite complexity and spine density and cell body size that chronic opiates produce in the mesolimbic system [59].

In summary, given that PTN, MK, and RPTPβ/ζ levels increase after acute morphine injection, return to basal levels during chronic opioid treatment, and are up-regulated again during morphine withdrawal, we hypothesize that signaling through these cytokines plays a role in mediating, at least in part, neuroprotective and behavioral adaptations that are observed during opiate addiction.

Compliance with Ethical Standards

Conflict of Interest The authors declare that they have no competing interests.

Authors' Contribution DG-P designed and performed the research, analyzed the data, and wrote the paper. MLL revised the manuscript. MVM conducted the astrocyte quantification and contributed to editing the paper.

References

1. Svendsen CN (2002) Neurobiology: the amazing astrocyte. Nature 417:29–32
2. Ullian EM, Sapperstein SK, Christopherson KS, Barres BA (2001) Control of synapse number by glia. Science 291:657–61
3. Beitner-Johnson D, Guitart X, Nestler EJ (1993) Glial fibrillary acidic protein and the mesolimbic dopamine system: regulation by chronic morphine and Lewis-Fischer strain differences in the rat ventral tegmental area. J Neurochem 61:1766–73
4. Watkins LR, Hutchinson MR, Johnston IN, Maier SF (2005) Glia: novel counter-regulators of opioid analgesia. Trends Neurosci 28:661–9
5. Fellin T, Carmignoto G (2004) Neurone-to-astrocyte signalling in the brain represents a distinct multifunctional unit. J Physiol 559:3–15
6. Bohn MC (2004) Motoneurons crave glial cell line-derived neurotrophic factor. Exp Neurol 190:263–75
7. Vesce S, Bezzi P, Volterra A (2001) Synaptic transmission with the glia. Physiology 16:178–84
8. Hutchinson MR, Coats BD, Lewis SS, Zhang Y, Sprunger DB, Rezvani N et al (2008) Proinflammatory cytokines oppose opioid induced acute and chronic analgesia. Brain Behav Immun 22:1178–89
9. Adler MW, Rogers TJ (2005) Are chemokines the third major system in the brain? J Leukoc Biol 78:1204–9

10. Rostene W, Kitabgi P, Parsadaniantz SM (2007) Chemokines: a new class of neuromodulator? Nat Rev Neurosci 8:895–903

11. Russo SJ, Dietz DM, Dumitriu D, Morrison JH, Malenka RC, Nestler EJ (2010) The addicted synapse: mechanisms of synaptic and structural plasticity in nucleus accumbens. Trends in Neurosci 33:267–76

12. Gonzalez-Castillo C, Ortuño-Sahagun D, Guzman-Brambila C, Pallas M, Rojas-Mayorquin AE (2014) Pleiotrophin as a central nervous system neuromodulator, evidences from the hippocampus. Front Cell Neurosci 8:443

13. Kadomatsu K, Muramatsu T (2004) Midkine and pleiotrophin in neural development and cancer. Cancer Lett 204:127–43

14. Mailleux P, Preud'homme X, Albala N, Vanderwinden JM, Vanderhaeghen JJ (1994) delta-9-Tetrahydrocannabinol regulates gene expression of the growth factor pleiotrophin in the forebrain. Neurosci Lett 175:25–7

15. Le Grevès P (2005) Pleiotrophin gene transcription in the rat nucleus accumbens is stimulated by an acute dose of amphetamine. Brain Res Bull 65:529–32

16. Flatscher-Bader T, Wilce PA (2008) Impact of alcohol abuse on protein expression of midkine and excitatory amino acid transporter 1 in the human prefrontal cortex. Alcohol Clin Exp Res 32:1849–58

17. Marchionini DM, Lehrmann E, Chu Y, He B, Sortwell CE, Becker KG et al (2007) Role of heparin binding growth factors in nigrostriatal dopamine system development and Parkinson's disease. Brain Res 1147:77–88

18. Ferrario JE, Taravini IRE, Mourlevat S, Stefano A, Delfino MA, Raisman-Vozari R et al (2004) Differential gene expression induced by chronic levodopa treatment in the striatum of rats with lesions of the nigrostriatal system. J Neurochem 90:1348–58

19. Herradón G, Pérez-García C (2013) Targeting midkine and pleiotrophin signaling pathways in addiction and neurodegenerative disorders: recent progress and perspectives. Br J Pharmacol 171:837–48

20. Muramatsu T (2002) Midkine and pleiotrophin: two related proteins involved in development, survival, inflammation and tumorigenesis. J Biochem 132:359–71

21. Deuel TF, Zhang N, Yeh HJ, Silos-Santiago I, Wang ZY (2002) Pleiotrophin: a cytokine with diverse functions and a novel signaling pathway. Arch Biochem Biophys 397:162–71

22. Polykratis A, Katsoris P, Courty J, Papadimitriou E (2005) Characterization of heparin affin regulatory peptide signaling in human endothelial cells. J Biol Chem 280:22454–61

23. Qi M, Ikematsu S, Maeda N, Ichihara-Tanaka K, Sakuma S, Noda M et al (2001) Haptotactic migration induced by midkine. Involvement of protein-tyrosine phosphatase zeta. Mitogen-activated protein kinase, and phosphatidylinositol 3-kinase. J Biol Chem 276:15868–75

24. Vicente-Rodríguez M, Pérez-García C, Gramage E, Herradón G (2013) Genetic inactivation of pleiotrophin but not midkine potentiates clonidine-induced alpha-2 adrenergic-mediated analgesia. Pharmacol Biochem Behav 110:185–91

25. Gramage E, Martín YB, Herradón G (2012) The heparin binding growth factors midkine and pleiotrophin regulate the antinociceptive effects of morphine through α(2)-adrenergic independent mechanisms. Pharmacol Biochem Behav 101:387–93

26. Di Chiara G, Imperato A (1988) Drugs abused by humans preferentially increase synaptic dopamine concentrations in the mesolimbic system of freely moving rats. Proc Natl Acad Sci U S A 85:5274–8

27. Ikemoto S (2007) Dopamine reward circuitry: two projection systems from the ventral midbrain to the nucleus accumbens-olfactory tubercle complex. Brain Res Brain Res Rev 56:27–78

28. García-Pérez D, Laorden ML, Nuñez C, Milanés MV (2014) Glial activation and midkine and pleiotrophin transcription in the ventral tegmental area are modulated by morphine administration. J Neuroimmunol 274:244–8

29. Frenois F, Cador M, Caille S, Stinus L, Le Moine C (2002) Neural correlates of the motivational and somatic components of naloxone-precipitated morphine withdrawal. Eur J Neurosci 16:1377–89

30. Houshyar H, Manalo S, Dallman MF (2004) Time-dependent alterations in mRNA expression of brain neuropeptides regulating energy balance and hypothalamo-pituitary-adrenal activity after withdrawal from intermittent morphine treatment. J Neurosci 24:9414–24

31. García-Pérez D, Sáez-Belmonte F, Laorden ML, Núñez C, Milanés MV, Milanés MV (2013) Morphine administration modulates expression of Argonaute 2 and dopamine-related transcription factors involved in midbrain dopaminergic neurons function. Br J Pharmacol 168:1889–901

32. Paxinos G, Watson C (2007) The rat brain in stereotaxic coordinates, 6th edn. Academic Press, Amsterdam

33. Raivich G, Bohatschek M, Kloss CUA, Werner A, Jones LL, Kreutzberg GW (1999) Neuroglial activation repertoire in the injured brain: graded response, molecular mechanisms and cues to physiological function. Brain Res Rev 30:77–105

34. Campbell LA, Avdoshina V, Rozzi S, Mocchetti I (2013) CCL5 and cytokine expression in the rat brain: differential modulation by chronic morphine and morphine withdrawal. Brain Behav Immun 34:130–40

35. Iseki K, Hagino S, Mori T, Zhang Y, Yokoya S, Takaki H et al (2002) Increased syndecan expression by pleiotrophin and FGF receptor-expressing astrocytes in injured brain tissue. Glia 39:1–9

36. Mourlevat S, Debeir T, Ferrario JE, Delbe J, Caruelle D, Lejeune O et al (2005) Pleiotrophin mediates the neurotrophic effect of cyclic AMP on dopaminergic neurons: analysis of suppression-subtracted cDNA libraries and confirmation in vitro. Exp Neurol 194:243–54

37. Taravini I, Chertoff M, Cafferata E, Courty J, Murer M, Pitossi F et al (2011) Pleiotrophin over-expression provides trophic support to dopaminergic neurons in parkinsonian rats. Molecular Neurodegeneration 6:40

38. Kim Y, Ryu J, Lee H, Lim I, Park D, Lee M et al (2010) Midkine, heparin-binding growth factor, blocks kainic acid-induced seizure and neuronal cell death in mouse hippocampus. BMC Neurosci 11:42

39. Hutchinson MR, Watkins LR (2013) Why is neuroimmunopharmacology crucial for the future of addiction research? Neuropharmacology 76(Pt B):218–27

40. Rock RB, Hu S, Sheng W, Peterson P (2006) Morphine stimulates CCL2 production by human neurons. J Neuroinflammation 3:32

41. Knapp DJ, Whitman BA, Wills TA, Angel RA, Overstreet DH, Criswell HE et al (2011) Cytokine involvement in stress may depend on corticotropin releasing factor to sensitize ethanol withdrawal anxiety. Brain Behav Immun 25(Supplement 1):S146–S154

42. Gramage E, Vicente-Rodríguez M, Herradón G (2015) Pleiotrophin modulates morphine withdrawal but has no effects on morphine-conditioned place preference. Neurosci Lett 604:75–9

43. Lorenzetto E, Moratti E, Vezzalini M, Harroch S, Sorio C, Buffelli M (2013) Distribution of different isoforms of receptor protein tyrosine phosphatase γ (Ptprg-RPTPγ) in adult mouse brain: upregulation during neuroinflammation. Brain Struct Funct 219:875–90

44. Hayashi N, Oohira A, Miyata S (2005) Synaptic localization of receptor-type protein tyrosine phosphatase zeta/beta in the cerebral and hippocampal neurons of adult rats. Brain Res 1050:163–9

45. Ferrario JE, Rojas-Mayorquín AE, Saldaña-Ortega M, Salum C, Gomes MZ, Hunot S et al (2008) Pleiotrophin receptor RPTP-ζ/β expression is up-regulated by L-DOPA in striatal medium spiny neurons of parkinsonian rats. J Neurochem 107:443–52

46. Rasmussen K, Beitner-Johnson DB, Krystal JH, Aghajanian GK, Nestler EJ (1990) Opiate withdrawal and the rat locus coeruleus: behavioral, electrophysiological, and biochemical correlates. J Neurosci 10:2308–17

47. Gramage E, Rossi L, Granado N, Moratalla R, Herradón G (2010) Genetic inactivation of pleiotrophin triggers amphetamine-induced cell loss in the substantia nigra and enhances amphetamine neurotoxicity in the striatum. Neuroscience 170:308–16

48. Gramage E, Putelli A, Polanco MJ, González-Martín C, Ezquerra L, Alguacil LF et al (2010) The neurotrophic factor pleiotrophin modulates amphetamine-seeking behaviour and amphetamine-induced neurotoxic effects: evidence from pleiotrophin knockout mice. Addict Biol 15:403–12

49. Sargeant TJ, Miller JH, Day DJ (2008) Opioidergic regulation of astroglial/neuronal proliferation: where are we now? J Neurochem 107:883–97

50. Johnson SW, North RA (1992) Opioids excite dopamine neurons by hyperpolarization of local interneurons. J Neurosci 12:483–8

51. Narita M, Miyatake M, Shibasaki M, Tsuda M, Koizumi S, Narita M et al (2005) Long-lasting change in brain dynamics induced by methamphetamine: enhancement of protein kinase C-dependent astrocytic response and behavioral sensitization. J Neurochem 93:1383–92

52. Jung CG, Hida H, Nakahira K, Ikenaka K, Kim HJ, Nishino H (2004) Pleiotrophin mRNA is highly expressed in neural stem (progenitor) cells of mouse ventral mesencephalon and the product promotes production of dopaminergic neurons from embryonic stem cell-derived nestin-positive cells. FASEB J 18:1237–9

53. Prediger R, Rojas-Mayorquin A, Aguiar A, Chevarin C, Mongeau R, Hamon M et al (2011) Mice with genetic deletion of the heparin-binding growth factor midkine exhibit early preclinical features of Parkinson's disease. J Neural Transm 118:1215–25

54. Ridet JL, Malhotra SK, Privat A, Gage FH (1997) Reactive astrocytes: cellular and molecular cues to biological function. Trends Neurosci 20:570–7

55. Pekny M, Nilsson M (2005) Astrocyte activation and reactive gliosis. Glia 50:427–34

56. Ahlemeyer B, Kölker S, Zhu Y, Hoffmann GF, Krieglstein J (2002) Increase in glutamate-induced neurotoxicity by activated astrocytes involves stimulation of protein kinase C. J Neurochem 82:504–15

57. Gramage E, Martín YB, Ramanah P, Pérez-García C, Herradón G (2011) Midkine regulates amphetamine-induced astrocytosis in striatum but has no effects on amphetamine-induced striatal dopaminergic denervation and addictive effects: functional differences between pleiotrophin and midkine. Neuroscience 190:307–17

58. Emeterio EP, Tramullas M, Hurlé MA (2006) Modulation of apoptosis in the mouse brain after morphine treatments and morphine withdrawal. J Neurosci Res 83:1352–61

59. Russo SJ, Mazei-Robison MS, Ables JL, Nestler EJ (2009) Neurotrophic factors and structural plasticity in addiction. Neuropharmacology 56(Supplement 1):73–82

60. Ciccarelli A, Calza A, Santoru F, Grasso F, Concas A, Sassoè-Pognetto M (2013) Morphine withdrawal produces ERK-dependent and ERK-independent epigenetic marks in neurons of the nucleus accumbens and lateral septum. Neuropharmacology 70:168–79

61. Li T, Hou Y, Cao W, Cx Y, Chen T, Sb L (2010) Naloxone-precipitated withdrawal enhances ERK phosphorylation in prefrontal association cortex and accumbens nucleus of morphine-dependent mice. Neurosci Lett 468:348–52

62. Hawes JJ, Brunzell DH, Narasimhaiah R, Langel U, Wynick D, Picciotto MR (2008) Galanin protects against behavioral and neurochemical correlates of opiate reward. Neuropsychopharmacology 33:1864–73

63. Berhow MT, Hiroi N, Nestler EJ (1996) Regulation of ERK (extracellular signal regulated kinase), part of the neurotrophin signal transduction cascade, in the rat mesolimbic dopamine system by chronic exposure to morphine or cocaine. J Neurosci 16:4707–15

64. Russo SJ, Bolanos CA, Theobald DE, DeCarolis NA, Renthal W, Kumar A et al (2007) IRS2-Akt pathway in midbrain dopamine neurons regulates behavioral and cellular responses to opiates. Nat Neurosci 10:93–9

65. Mazei-Robison MS, Koo JW, Friedman AK, Lansink CS, Robinson AJ, Vinish M et al (2011) Role for mTOR signaling and neuronal activity in morphine-induced adaptations in ventral tegmental area dopamine neurons. Neuron 72:977–90

66. Mi R, Chen W, Höke A (2007) Pleiotrophin is a neurotrophic factor for spinal motor neurons. Proc Natl Acad Sci U S A 104:4664–9